Local mean field approximation applied to a 3D spin crossover nanoparticles configuration: free energy analysis of the relative stability of the stationary states

C. Cazelles, Jörge Linares, Y. Singh, Pierre-Richard Dahoo, K. Boukheddaden

Local mean field approximation applied to a 3D spin crossover nanoparticles configuration: free energy analysis of the relative stability of the stationary states

C. Cazelles[1], J. Linares[2,3,*] ,Y. Singh[2], , P.-R. Dahoo[4] , K. Boukheddaden[2]
[1] Université Paris-Saclay, UVSQ, IUT de Mantes-en-Yvelines, 78200 Mantes-la-Jolie
[2] Université Paris-Saclay, UVSQ, CNRS, GEMaC, 78000, Versailles, France
[3] Departamento de Ciencias, Sección Física, Pontificia Universidad Católica del Perú, Apartado 1761 - Lima, Peru
[4]Université Paris-Saclay, UVSQ, CNRS, LATMOS, 78280, Guyancourt, France

*E-mail: jorge.linares@uvsq.fr

Abstract. The local mean field approximation is applied to an inhomogeneous 3D spin crossover (SCO) nanoparticle configuration with a special focus on its systemic effect on molecules which are localized in the bulk, at the corner, at the edge and at the surface. The matrix effect at the surface is introduced through a specific interaction term, L. The partition function for each region allows the determination of the total free-energy F from which the stability of each configuration is analyzed through thermodynamic considerations.

Keywords: Spin-crossover, nanoparticles, mean field approximation, phase transition, matrix effect

1.Introduction

Fe(II) Spin-crossover (SCO) shows a particular first-order phase transition, with thermal hysteresis [1-5] that is mediated between two spin states, Low-Spin (LS) with degeneracy g_{LS} , stable at low temperatures and High-Spin (HS) with degeneracy g_{HS} (> g_{LS}), stable at high temperatures. Between two temperatures, namely termed T_{down} and T_{up} a SCO molecule can be in one of these two states depending on its thermal history. This "bi-stable" character is the result of the competition between the ligand field energy acting on each spin-state and the elastic interactions between the molecules.

2. Model

In the framework of the Ising-like model [6-11] each SCO molecule is described by a two-level fictitious spin having two eigenvalues $s = +1$ and $s = -1$, respectively associated with the HS and LS states. The total Hamiltonian of a system of N_T molecules, taking into account the short (J) - and long-range (G) interactions, as well as the matrix effect (L), is expressed as:

$$H = \frac{\Delta - k_B T \ln g}{2} \sum_{i=1}^{N_T} \sigma_i - J \sum_{<i,j>} \sigma_i \sigma_j - G \sum_{i=1}^{N_T} \sigma_i < \sigma > - L \sum_{i=1}^{M} \sigma_i \quad (1)$$

where g = g_{HS}/g_{LS} , $\Delta\ (> 0)$ is the energy difference between the (HS) and (LS) states, T is the absolute temperature, k_B is the Boltzmann constant, and M is the total number of molecules located at the surface.

In this contribution, the local mean-field approximation (LMFA) [12] which consists in replacing the spin state of each neighbor by its mean value is applied. Accordingly, the short (J)- and the long (G) range interactions are replaced by only one coupling interaction Γ. The global Hamiltonian of the system can then be re-written as follows:

$$H = \frac{\Delta - k_B T \ln g}{2} \sum_{i=1}^{N_t} \sigma_i - \Gamma < \sigma > \sum_{i=1}^{N_T} q_i \sigma_i - L \sum_{i=1}^{M} \sigma_i \qquad (2)$$

where q_i denotes the number of interactions between a molecule and its first-neighbors. Fig 1 is a schematic view of a 3D SCO nanoparticle configuration.

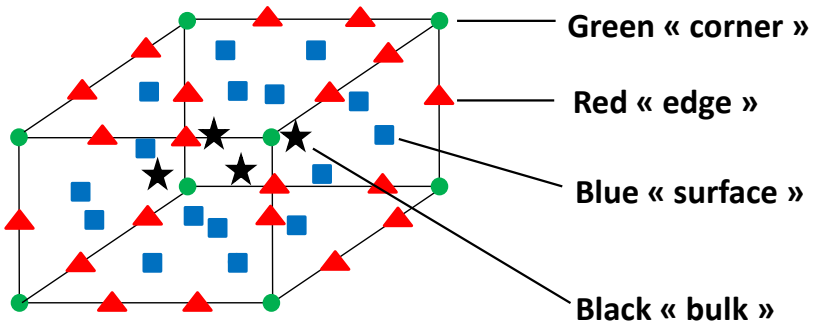

Figure 1. Schematic view of the 4x4x3 lattice of a SCO nanoparticle: filled black stars represent bulk sites (N_b), while blue squares, red triangles and green circles represent respectively surface (N_s), edge (N_e) and corner (N_c) sites.

Four types of sites are depicted: molecules located in the bulk N_b, on the surface N_s, on the edge N_e and on the corner N_c. The Hamiltonian can finally be expressed as follows:

$$H = \frac{\Delta - k_B T \ln g}{2} \sum_{i=1}^{N_T} \sigma_i - \sum_{i=1}^{N_T} \frac{-2\Gamma q_i < \sigma > -2 z_i L}{2} \sigma_i = -\sum_{i=1}^{N_T} h_i \sigma_i \qquad (3)$$

where, the effective field "h_i" is given by :

$$h_i = -\frac{\Delta - k_B T \ln g - 2\Gamma q_i < \sigma > -2 z_i L}{2} \qquad (4)$$

and z_i denotes the number of interactions between a molecule and the environment (surface pending links). The values of q_i and z_i are listed in Table 1 for the case $N_x, N_y \text{ and } N_z \geq 3$

Table 1. Number of interactions as a function of the molecule's position in the lattice for the case $N_x, N_y \text{ and } N_z \geq 3$

Site	bulk	surface	edge	corner
q_i	6	5	4	3
z_i	0	1	2	3

The partition function for this inhomogeneous mean-field system writes
$Z = Z_b^{N_b} Z_c^{N_c} Z_e^{N_e} Z_s^{N_s}$

with the general expressions for the partition functions for each of the four regions given by:

$$Z_\alpha = 2 \cosh \beta \left(\frac{\Delta - k_B T \ln g - 2\Gamma q_\alpha < \sigma > -2 z_\alpha L}{2} \right) \qquad (5)$$

where $\alpha = b, c, e, s$, takes its corresponding value according to the position of the site in the lattice and

$$< \sigma > = \frac{N_b < \sigma_b > + N_c < \sigma_c > + N_e < \sigma_e > + N_s < \sigma_s >}{N_{tot}} = \frac{1}{N_{tot}} \sum_{\alpha} N_\alpha < \sigma_\alpha > \quad (6)$$

In compact form, the total free energy F is written as:

$$F = \sum_{\alpha=b,c,e,s} \left(\frac{q_\alpha N_\alpha}{2N_{tot}} \Gamma < \sigma_\alpha >^2 - k_B T \ln Z_\alpha \right) \quad (7)$$

where, the first term is the "correction term" due to the mean-field approximation.

At thermal equilibrium characterized by, $\frac{\partial F}{\partial <\sigma_\alpha>} = 0 \quad (\alpha = b, c, e, s)$, the following set of self-consistent equations are calculated:

$$< \sigma_\alpha > = -\tanh \beta \left[\frac{\Delta - k_B T \ln g - 2\Gamma q_\alpha < \sigma > - 2 z_\alpha L}{2} \right], \text{with } \alpha = b, c, e, s. \quad (8)$$

The average "magnetization" of the system, from which the HS fraction is determined, is given by the relation:

$$< \sigma > = \frac{1}{N_{tot}} \sum_{\alpha} N_\alpha < \sigma_\alpha >, \quad (9)$$

3.Results and Discussion

Simulations are performed with parameter values that are chosen from experimental data of typical SCO solids characterized by: Δ/k_B=3126 K, ln(g)= 8.45. Figure 2 shows the thermal evolution of the average high spin fraction Nhs defined as $Nhs = \frac{1+<\sigma>}{2}$, thus showing the existence of a thermal hysteresis behavior (thermal bistability) in the temperature interval between 327K and 353 K. In contrast, in the low-and high-temperature regions corresponding respectively to T<327 K and T > 353 K, the system occupies the respective LS-state ($< \sigma >$ close to -1) and HS ($< \sigma >$ is close to +1) state.

Fig 3 shows the thermal evolution of the free-energy per site of the system. The minima values of this free-energy F are the stables states which are represented as red circles in Fig 2. In the Fig 2 and 3, the black triangles and blue stars represent respectively the unstable states and the metastable states termed *m*.

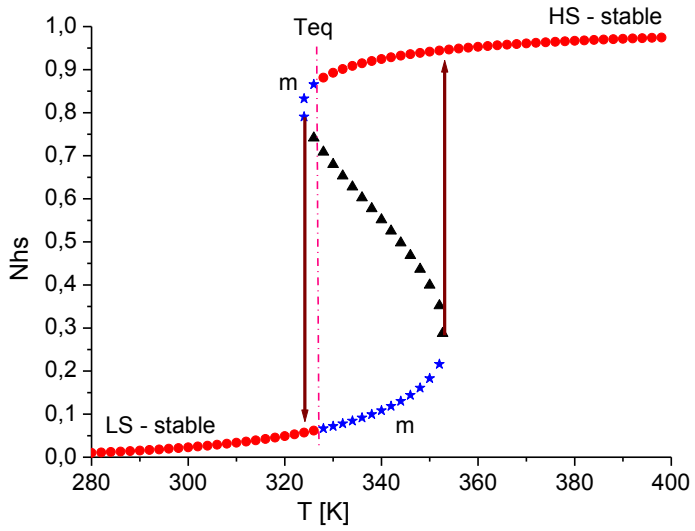

Figure 2. Evolution of the (HS) molar fraction N_{HS} as a function of temperature for a 3D SCO cubic lattice with size 8×8×8 (512 molecules) showing the stable (red circles), metastable *m* (blue stars) and unstable (black up triangles) states. The parameter values are Δ/k_B=3126 K, Γ/k_B=100 K, L/k_B=150 K and ln(g)=8.45.

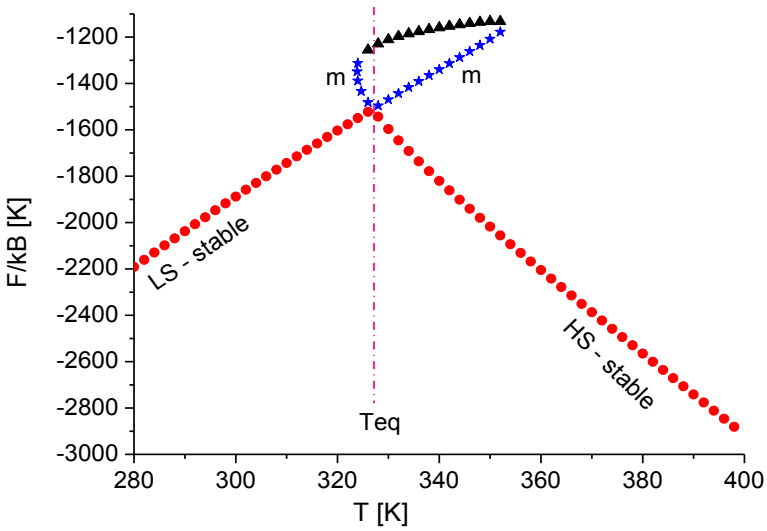

Figure 3. Free-Energy F versus T corresponding to the parameter values used for Fig 2. Red circles, blue stars and black up triangles represent respectively the stable, metastable *m* and unstable states.

On the basis of the equation (7) the Free-Energy F has been calculated for each solution represented in Fig 2. The stable solutions correspond to those with the minimum value of F. It is interesting to notice that while in most usual Ising models, the transition temperature, Teq, locates in the middle of the thermal hysteresis, Fig. 3 shows that for the present case, the effect of interactions of different characteristics results in a shift of the transition temperature towards the lower switching temperature. Consequently, this effect allows one to fix the stable as well as the metastable solutions inside the thermal hysteresis.

Among the various potentialities of this model, Fig 4 shows a particular case obtained with the interaction parameter values, Δ/k_B=3126 K, Γ/k_B=147 K, L/k_B=730 K and ln(g)=8.45, leading to the simulation of multi-step transitions. Indeed, when T is between T_1= 237 K and T_2= 248 K, a three state case is possible, where the intermediate state is due to the coexistence of HS and LS species.

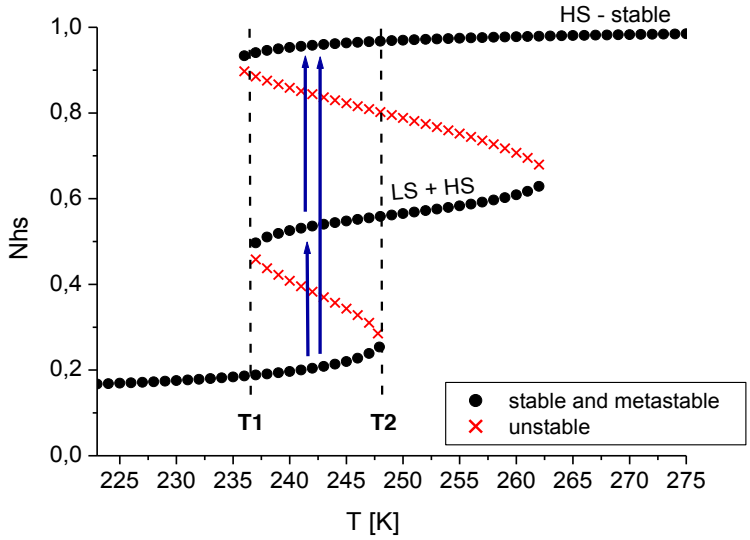

Figure 4. Evolution of the (HS) molar fraction as a function of temperature showing three states hysteresis loop in a 3D SCO cubic lattice with size 8×8×8. Black circles correspond to the stable and metastable regions and red crosses are the unstable regions. The computational parameters are Δ/k_B=3126 K, Γ/k_B=147 K, L/k_B=730 K and ln(g)=8.45.

4. Conclusion

This work demonstrates that the local mean-field approximation, applied in the framework of the Ising-like model, is well suited to perform calculations on SCO nanoparticles configurations partitioned in terms of interactions of different types. Thus, four regions are depicted, namely in the bulk, at the corner, at the edge and at the surface with SCO molecules characterized by different numbers of neighbors and interaction types. Matrix effects have also been taken specifically into account. The additive free-energy F has been calculated so as to analyze the stability of each solution from the thermodynamics. In addition to the first-order transition that is accompanied with a thermal hysteresis, three-states transitions have also been simulated, and which is the result of the competition between the environmental effect and the internal elastic interactions.

5. REFERENCES

1. Gütlich P., Struct. Bond. **1981**, 44, 83–195
2. Gütlich P., Hausser A., Coord. Chem. Rev. 1990, 97, 1-22
3. Varret F., Salunke S.A., Boukheddaden K., Bousseksou A., Codjovi E., Enachescu C., Linares J., Comptes Rendus Chimie 6 (3), 2003, 385-393
4. Enachescu C., Menendez N., Codjovi E., Linares J., Varret F., Stancu A., Physica B: Condensed Matter 306 (1-4), 2001, 155-160
5. Rotaru A., Dîrtu M.M., Enachescu C., Tanasa R., Linares J., Stancu,A. Garcia Y., Polyhedron 28 (13), 2531-2536
6. Wajnflasz J., Pick R., Phys. Colloques, 32, 91-92 (1971)
7. Bousseksou A., Nasser J., Linares J., Boukheddaden K., Varret F., J. Phys I Fr, 1992, 2, 1381-1403
8. Muraoka A., Boukheddaden K., Linares J., Varret F., Phys. Rev. B, 84, 054119 (2011)
9. Linares J., Enachescu C., Boukheddaden K., Varret F., Polyhedron 22 (14-17), 2453-2456
10. Linares J., Jureschi C.M., Boukheddaden K., Magnetochemistry, 2016, 2(2), 24
11. Chiruta D., Jureschi C.M., Linares J., Garcia Y., Rotaru A., Journal of Applied Physics 115 (5), 053523

12. Allal S.E., Linares J., Boukheddaden K., Dahoo P.R., De Zela F., Journal of Physics SC, 936 (2017) 012052,